

Supporting Information

Enhanced photocatalytic H₂ evolution over covalent organic framework through assembled NiS cocatalyst

Hualei Zhang,* Zheng Lin, and Jia Guo*

State Key Laboratory of Molecular Engineering of Polymers, Department of
Macromolecular Science, Fudan University, Shanghai 200438, China.

*E-mail: 18110440049@fudan.edu.cn; guojia@fudan.edu.cn.

Section I. Materials and Methods

1. Materials

Anhydrous 1,2-dichlorobenzene (o-DCB), anhydrous n-butanol (n-BuOH) and chloroplatinic acid hexahydrate were purchased from Aladdin Industrial. Tetrahydrofuran (THF), acetone, Sodium sulfide nonahydrate, Sodium Sulfite, L(+)-Ascorbic acid and Nickel(II) acetate tetrahydrate were purchased from Shanghai Chemical Regents Company. Methyl Alcohol, Ethanol, Triethanolamine and Ascorbic acid were purchased from Sinopharm Chemical Reagent Co. Ltd. 1,3,5-Triformylphloroglucinol (Tp) and 4,4'-biphenyldiamine (BD) were purchased from Jilin Chinese Academy of Sciences-Yanshen technology Co. Ltd. Ascorbic acid were purchased from Sinopharm Chemical Reagent Co. Ltd. All the chemicals were used without further purification.

2. Characterizations

Powder X-ray diffraction (PXRD) patterns were collected at room temperature on an X-ray diffraction spectrometer (Bruker D8 Advance, Germany) with Cu K α radiation at $\lambda = 0.154$ nm operating at 40 kV and 40 mA. Fourier transform infrared (FT-IR) spectra were recorded on Nicolet 6700 (ThermoFisher, USA) Fourier transformation infrared spectrometer. Solid-state CP/MAS ^{13}C NMR spectra were recorded on 400WB AVANCE III (Bruker, Switzerland) plus 400 MHz spectrophotometer at 298 K. High-resolution transmission electron microscopy images were obtained using a JEOL 2100F microscope operated at 200 kV accelerating voltage. The elemental mappings of C, N, O and S atoms were collected using the same transmission electron microscope (operating at 200 kV) under the ADF STEM mode. The chemical compositions of samples were examined using X-ray photoelectron spectroscopy (XPS) with Thermo Scientific K-Alpha+. All the XPS spectra were corrected according to C 1s line at 284.6 eV. Diffuse reflectance UV-visible absorption spectra were collected on a Lambda 750 spectrometer (referenced to barium sulphate). On the basis of the Kubelka-Munk (KM) method and the UV visible diffuse absorption spectra by the following equation:

$$\alpha_{hv} = A(hv-E_g)^2,$$

the E_g of all samples can be calculated experimentally, where α , A , h , and $h\nu$ are the absorption coefficient, constant, and Planck's constant, and photon energy, respectively. Photoluminescence (PL) profiles were performed on Fluorescence Spectrophotometer Qm 40 (PTI, USA) with a 350 nm laser excitation source. The lifetimes of fluorescence spectra was examined by FLS1000 (Edinburgh Instruments, UK) equipped with a 350 nm laser as the excitation source and employing Time Correlated Single Photon Counting (TCSPC) technique. Inductively coupled plasma atomic emission spectroscopy (ICP-AES) was done on a VARIAN VISTA RL simultaneous spectrometer (Agilent Technologies, Santa Clara, California, USA) with a CCD-detector. Nitrogen sorption isotherms were determined at 77 K using the Quantachrome Autosorb-iQ after more than 8 hours of degassing in vacuum at 120 °C.

3. Methods

3.1 Electrochemical measurements

Electrochemical measurements were measured by CHI760E electrochemical workstation (Chenhua, Shanghai) in a three electrode cell system. The COF powder was ultrasonically dispersed in ethanol for 10 min. Then the dispersion was drop-cast onto the fluorine-doped tin oxide (FTO) conductive glass for the preparation of the working electrode. The Ag/AgCl electrode worked as the reference electrode while the platinum wire worked as the counter electrode. The Mott-Schottky tests were carried out in 0.1 M Na_2SO_4 solution as the supporting electrolyte. All of the potentials were calibrated to the Reversible Hydrogen Electrode (RHE). Photocurrent measurements were performed using a 300 W Xe lamp with a cutoff filter ($\lambda \geq 420$ nm). Electrochemical impedance spectroscopy (EIS) were measured in 0.1 M NaCl solution.

Section II. Supplementary figures and tables

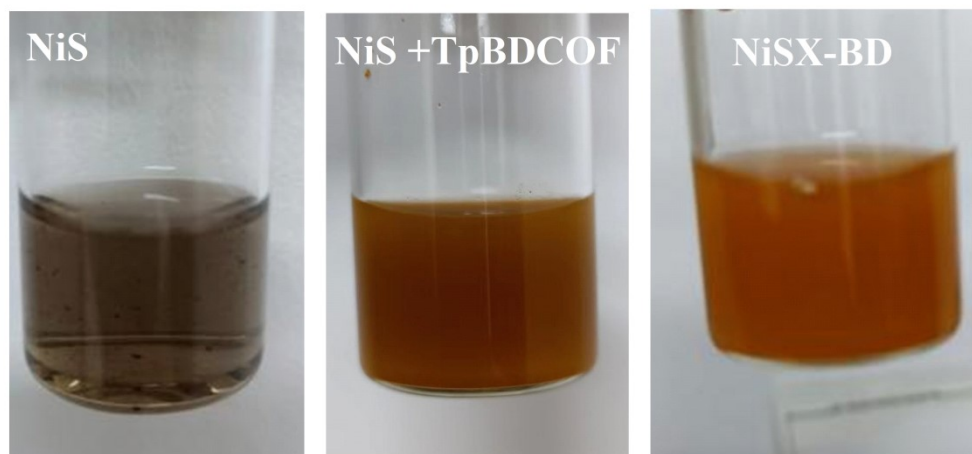


Figure S1. The synthetic experiment of NiSX-BD.

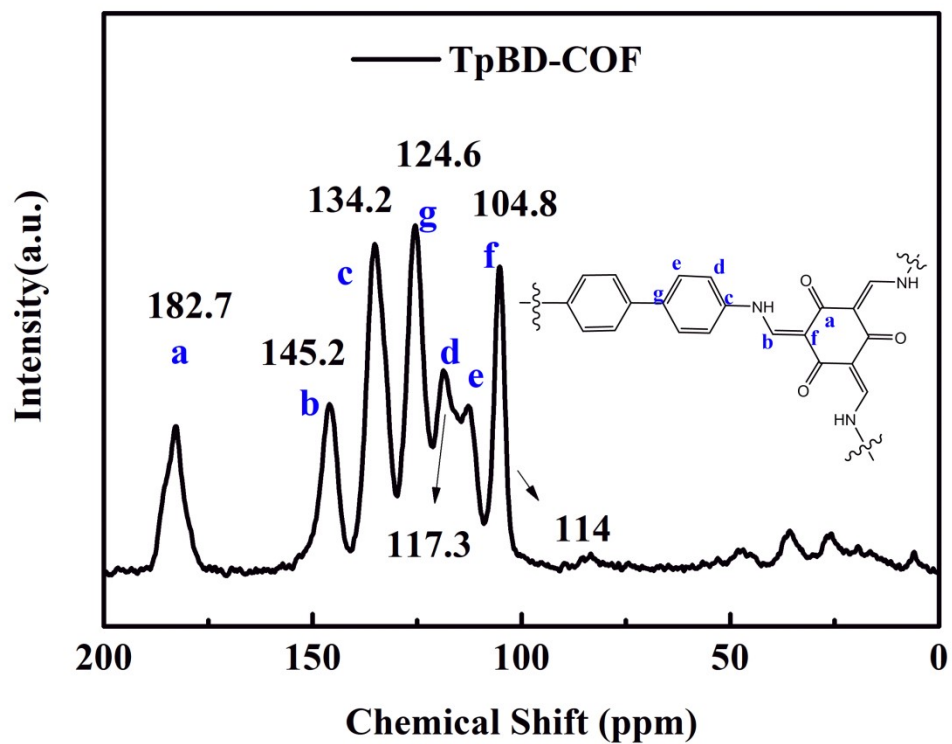


Figure S2. Solid-state ^{13}C NMR spectrum of the TpBD-COF.

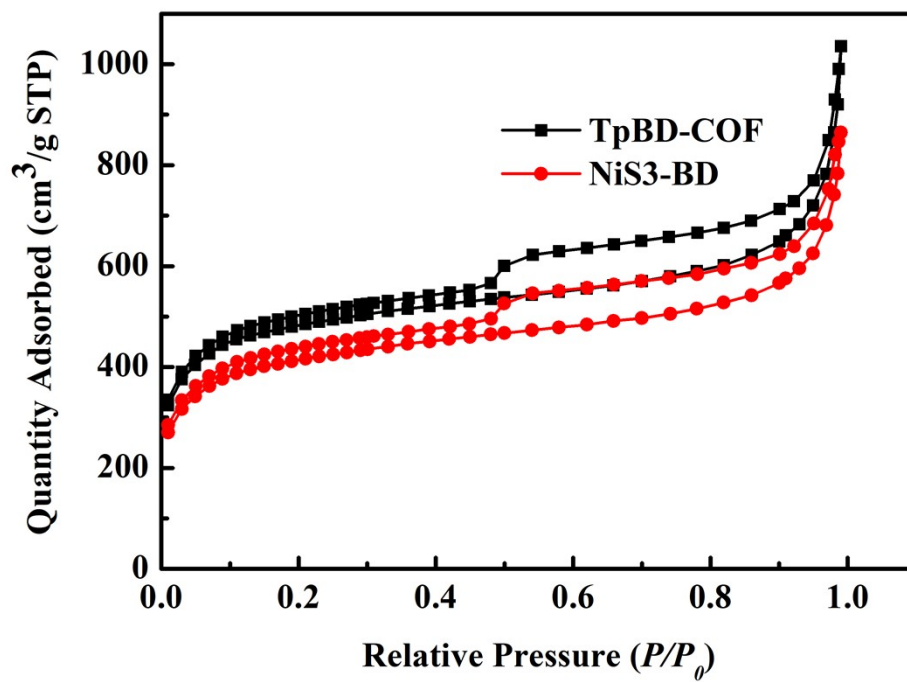


Figure S3. N₂ adsorption (closed circles) and desorption (open circles) isotherms (77 K) of the TpBD-COF and NiS3-BD.

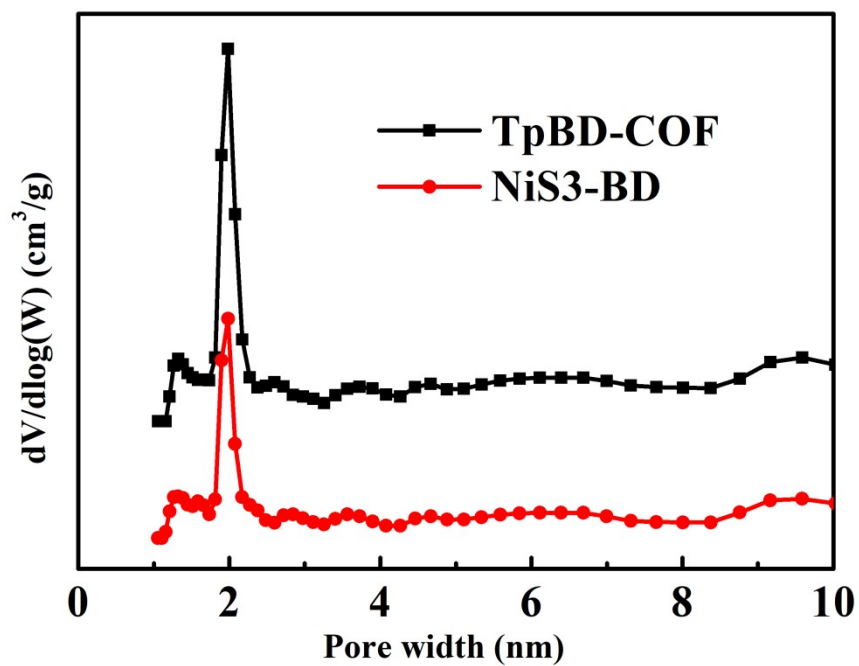


Figure S4. Pore-size distributions of TpBD-COF and NiS3-BD.

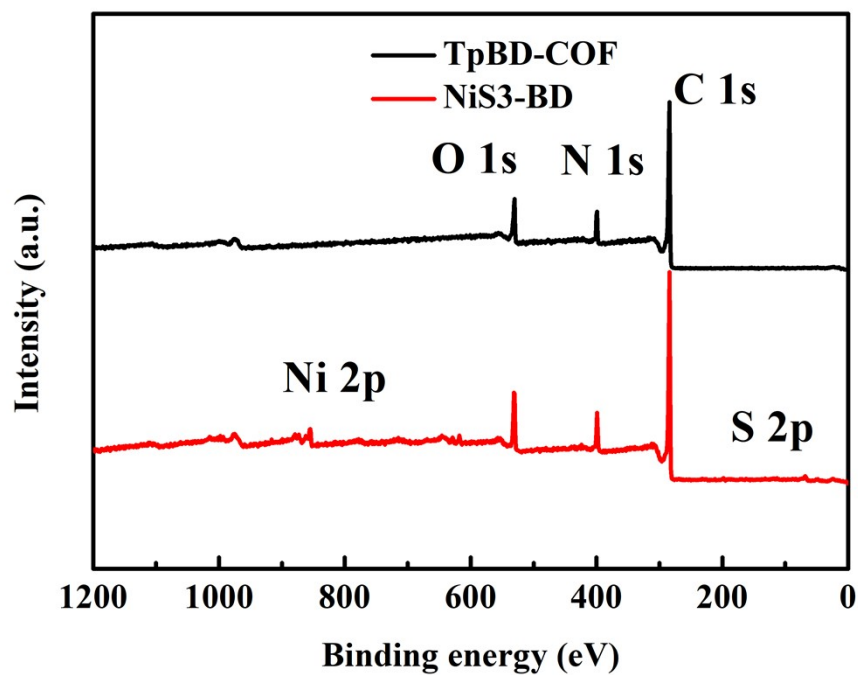


Figure S5. XPS survey spectrum of TpBD-COF and NiS3-BD.

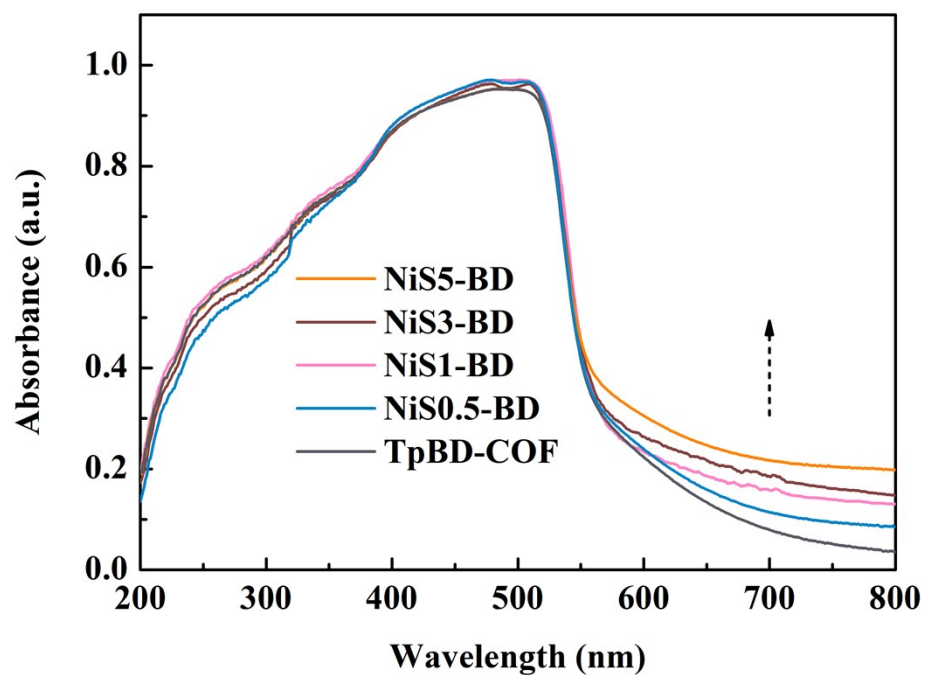


Figure S6. UV-vis diffuse reflectance spectroscopy of TpBD-COF and NiSX-BD.

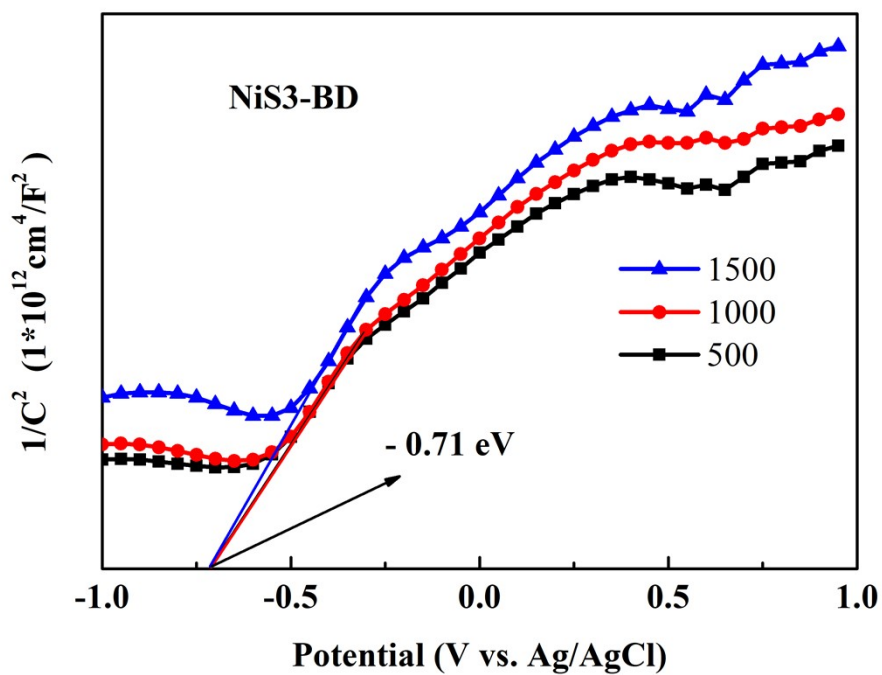


Figure S7. Mott-Schottky plots of the NiS₃-BD.

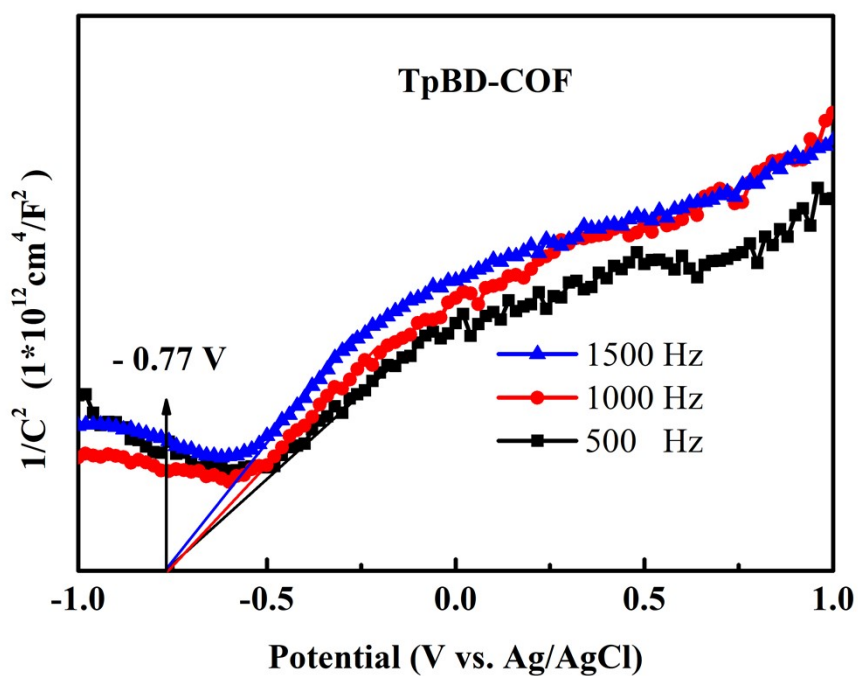


Figure S8. Mott-Schottky plots of the TpBD-COF.

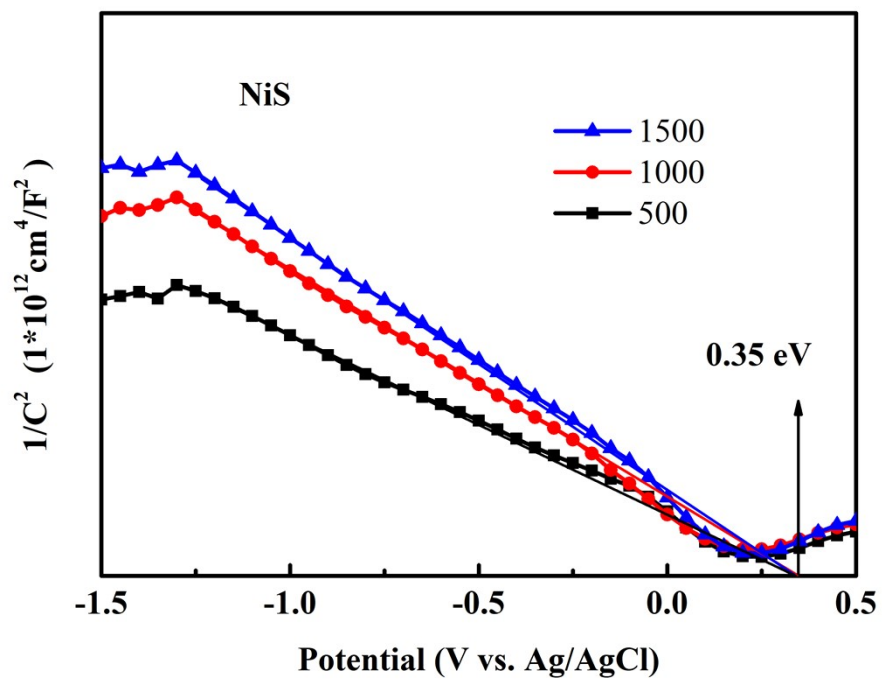


Figure S9. Mott-Schottky plots of the NiS.

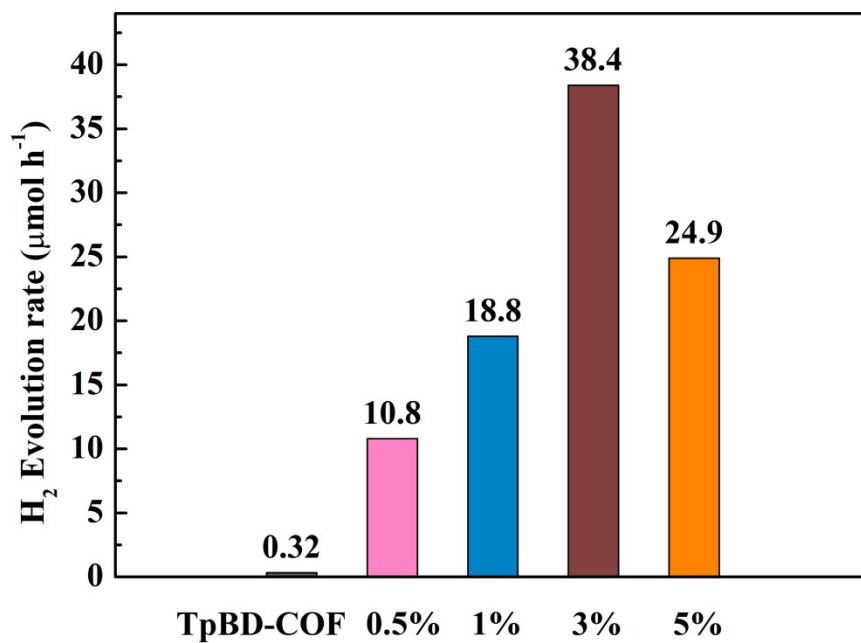


Figure S10. Average photocatalytic H₂ evolution rate of TpBD-COF and NiSX-BD photocatalysts with varying NiS loading.

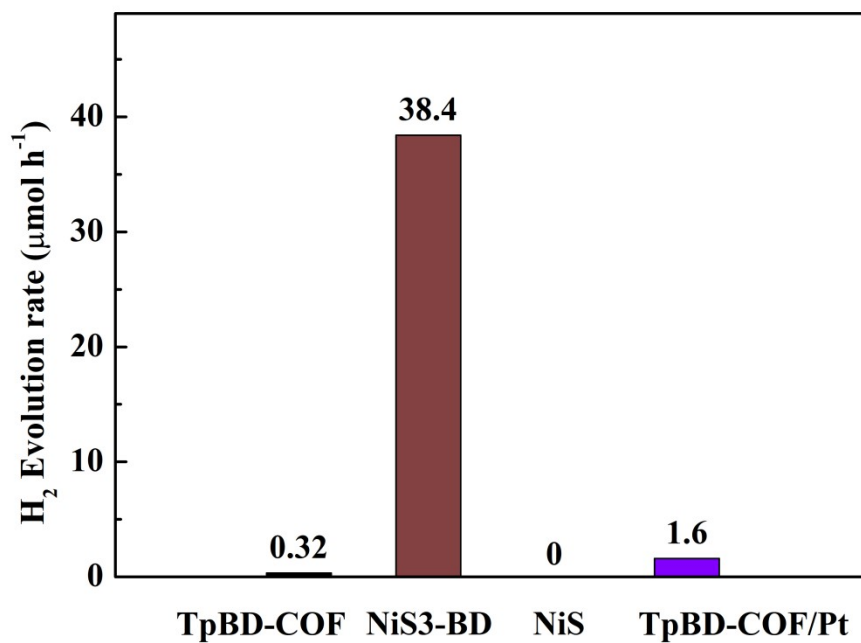


Figure S11. Average photocatalytic H₂ evolution rate of TpBD-COF, NiS₃-BD, NiS, and TpBD-COF/Pt.

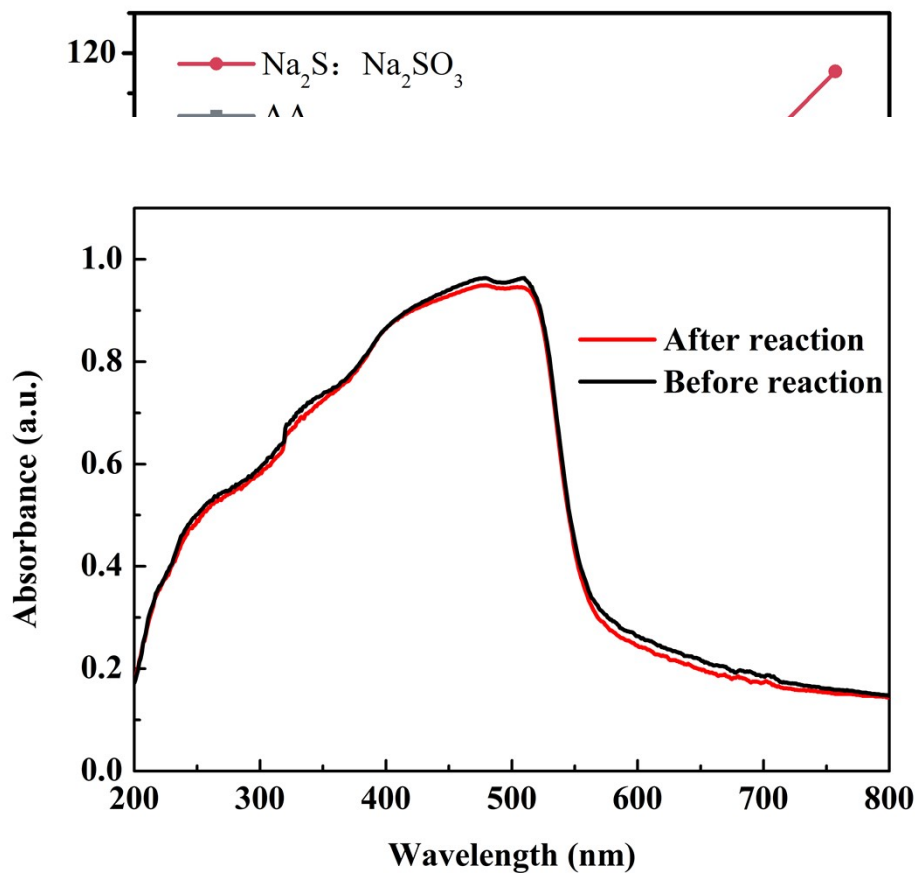


Figure S12. Photocatalytic hydrogen production performance of NiS3-BD measured in the presence of different hole scavengers.

Figure S13. FT-IR spectra of NiS3-BD before (black) and after 18h (red) photocatalytic process.

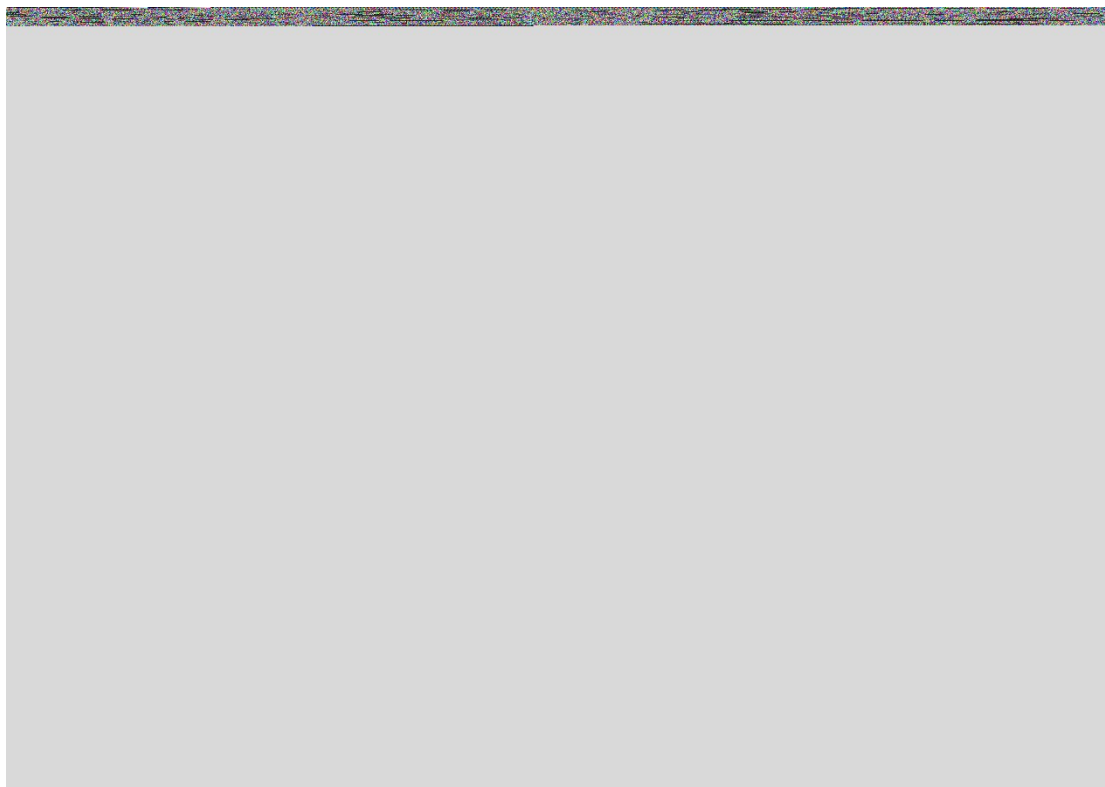


Figure S14. UV-vis diffuse reflectance spectroscopy of NiS₃-BD before (black) and after 18h (red) photocatalytic process measured in the solid state.

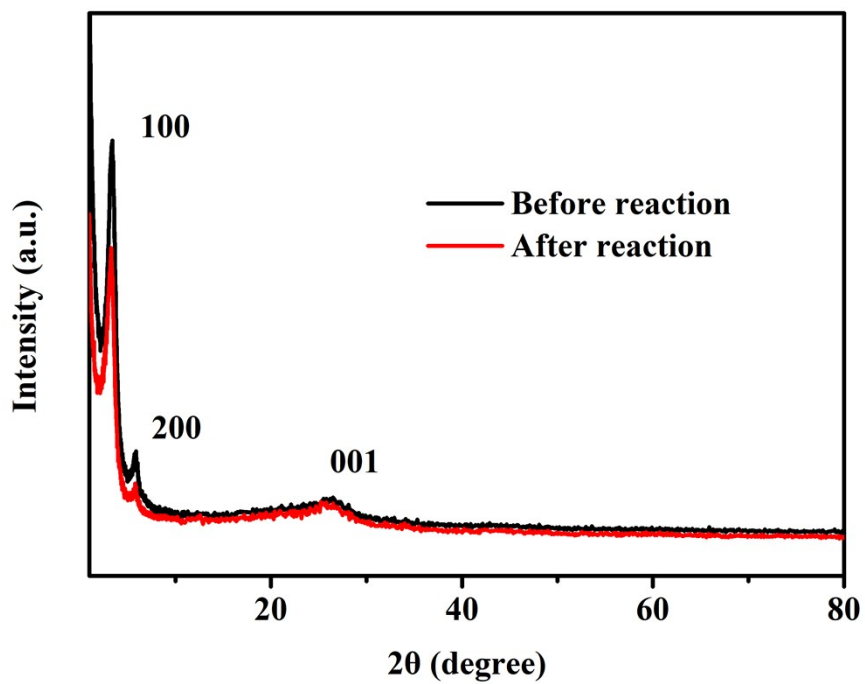


Figure S15. Experimental powder X-ray diffraction pattern of the raw NiS₃-BD (black), and the NiS₃-BD photocatalyst after 18 h hydrogen evolution experiment under visible light (red).

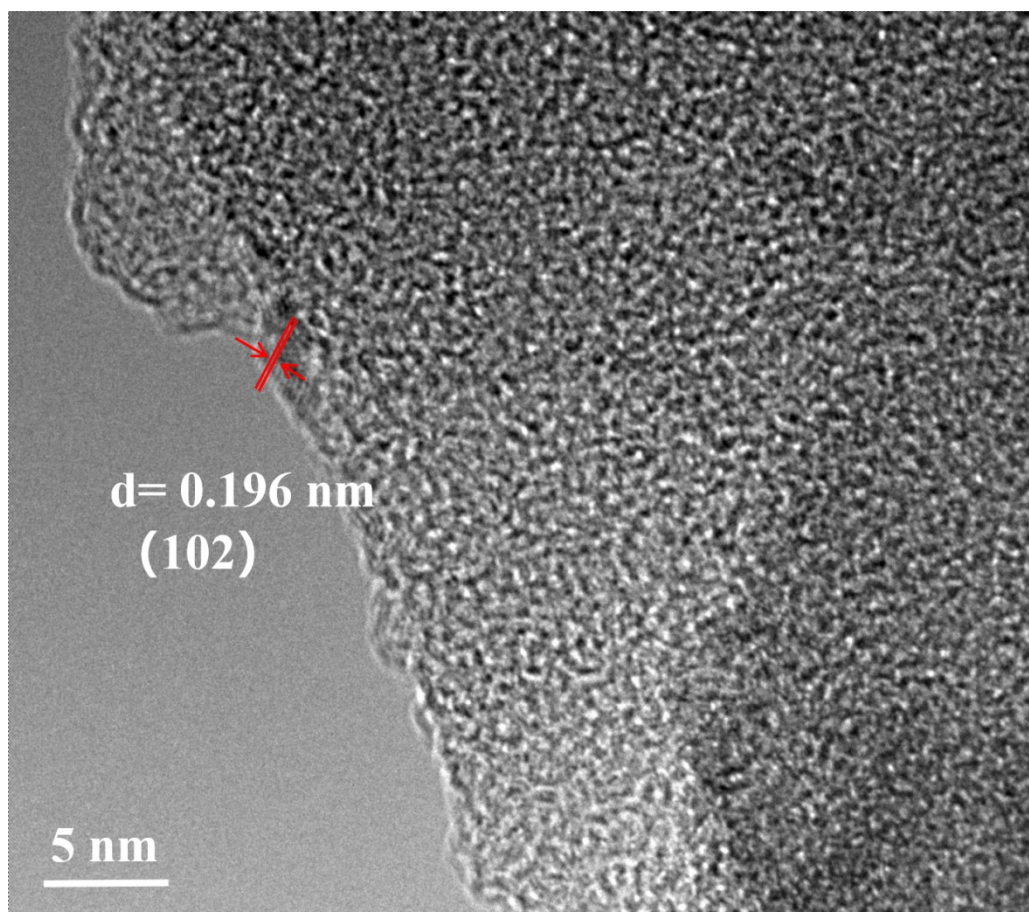


Figure S16. HR TEM image of NiS₃-BD after photocatalytic reaction.

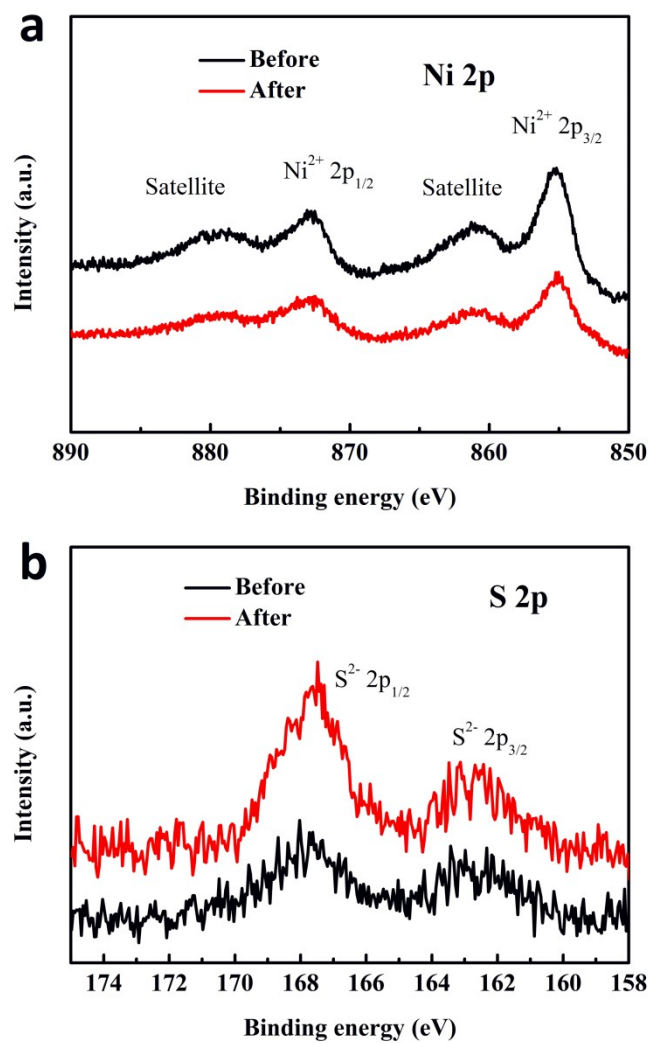


Figure S17. XPS of the NiS₃-BD after the photocatalytic hydrogen production: a) Ni 2p peak; b) S 2p peak.

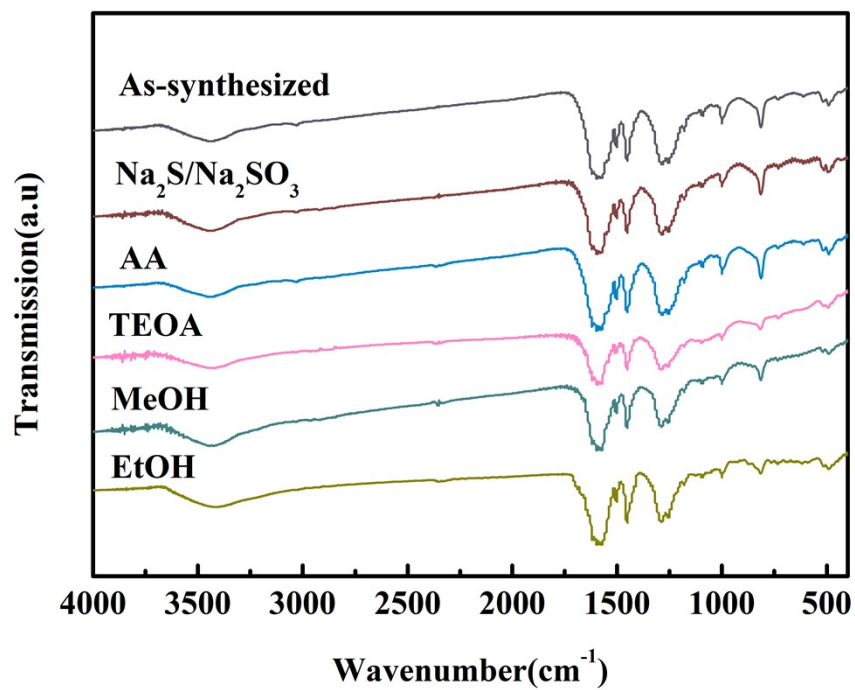


Figure S18. FT-IR spectra of the TpBD-COF and immersed in solution with different sacrificial agents for 2 days.

Table S1. ICP-AES of NiSX-BD.

	NiS0.5-BD	NiS1-BD	NiS3-BD	NiS5-BD
Ni wt%	0.31	0.62	1.91	3.14
S wt%	0.17	0.33	1.01	1.69

Table S2. Summary of H₂ evolution activity of photocatalysts.

Catalyst	Co-catalyst	SED	Illumination	Activity, μmol g⁻¹ h⁻¹	AQE 420 nm	Ref
TpBD-COF	NiS	Na₂S/ Na₂SO₃	> 420 nm	3840	0.24%	This work
g-C ₃ N ₄ /CdS	NiS	TEOA	> 420 nm	2563	-	[1]
TMC/NiS-1.5	NiS	LA	Xe lamp	638	-	[2]
Ni(OH) ₂ -2.5%/TpPa-2	Ni(OH) ₂	SA	> 420 nm	1895.99	-	[3]
TpPa-1-COF	MoS ₂	AA	> 420 nm	5585	0.76%	[4]
SnS ₂ /TpPa-1-COF	-	AA	> 420 nm	2474	0.23%	[5]
FS-COF	Pt	AA	> 420 nm	10100	3.2%	[6]
N ₂ -COF	Co-1 ^a	TEOA	AM1.5	782	0.16%	[7]
N ₂ -COF	Co-2 ^b	TEOA	AM1.5	414	-	[7]
N ₂ -COF	Co-1	TEOA	AM1.5	100	-	[7]
N ₂ -COF	Co-1	TEOA	AM1.5	163	-	[7]
COF-42	Co-1	TEOA	AM1.5	233	-	[7]
CdS-COF	Pt	LA	> 420 nm	3678	4.2	[8]
Tp(BT0.05TP0.95)-COF	Pt	AA	> 420 nm	9840	2.34%	[9]
SP ² -COF _{ERDN}	Pt	TEOA	> 420 nm	2120	0.47%	[10]
TpDTz COF	NiME	TEOA	AM 1.5	941	0.2%	[11]

AA: Ascorbic Acid, SA: Sodium ascorbate, TEOA: Triethanolamine, LA: lactic acid:

Co-1^a: [Co(dmgH)₂pyCl], Co-2^b: [Co(dmgBF₂)₂(OH₂)₂].

References

- 1 J. Yuan, J. Wen, Y. Zhong, X. Li and Y. Fang, *J. Mater. Chem. A.*, 2015, **3** (35): 18244-18255.
- 2 L. Zhang, B. Z Tian, F. Chen and J. L Zhang, *Int. J. Hydrogen. Energy.*, 2012, **37** (22): 17060-17067.
- 3 H. Dong, X. B. Meng, X. Zhang, H. L. Tang and J. W. Liu, *Chem. Eng. J.*, 2020, **379**: 122342.
- 4 M. Y. Gao, C. C. Li, H. L. Tang, X. J. Sun and H. Dong, *J. Mater. Chem. A.*, 2019, **7**, 20193-20200.
- 5 D. Shang, D. Li, B. Chen, B. Luo, Y. Huang and W. Shi, *ACS. Sustain. Chem. Eng.*, 2021, **9**, 14238-14248.
- 6 X. Y. Wang, L. J. Chen, M. A. Zwijnenburg, R. S. Sprick R and I. A. Cooper, *Nat. Chem.*, 2018, **10**, 1180-1189.
- 7 T. Banerjee, F. Haase, G. Savasci, K. Gottschling and C. Ochsenfeld, *J. Am. Chem. Soc.*, 2017, **139** (45): 16228-16234.
- 8 T. Jayshri, B. A. Harshitha, D. Aparna, D. D. David and K. Sreekumar, *Chem. Eur. J.*, 2014, **20** (48): 15961-15965.
- 9 T. Zhou, X. Huang, Z. Mi, Y. Zhu, C. C. Wang and J. Guo, *Poly. Chem.*, 2021, **12**, 250-3256.
- 10 E. Q. Jin, Z. A. Lan, Q. H. Jiang, X. C. Wang and D. L. Jiang, *Chem*, 2019, **5**, 1632-1647.
- 11 B. P. Biswal, G. H. V Gonzalez, T. Banerjee, L. Grunenberg and G. Savasci, *J. Am. Chem. Soc.*, 2019, **141**, 11082-11092.